DALTON
FULL PAPER

[*Triangulo*-Hg_3(μ-dppm)$_3$](O_3SCF_3)$_4$: first complete NMR analysis of a homoleptic [M_3(μ-dppm)$_3$] type system and study of the conformation dynamics in solution by use of its dpam/mdppm derivatives

Walter Schuh,[a] Gerhard Hägele,*[b] Ralf Olschner,[b] Andreas Lindner,[b] Peter Dvortsak,[c] Holger Kopacka,[a] Klaus Wurst[a] and Paul Peringer *[a]

[a] *Institut für Allgemeine, Anorganische und Theoretische Chemie, Universität Innsbruck, Innrain 52a, A-6020 Innsbruck, Austria. E-mail: paul.peringer@uibk.ac.at*
[b] *Institut für Anorganische und Strukturchemie, Heinrich Heine Universität Düsseldorf, Universitätsstraße 1, D-40225 Düsseldorf, Germany. E-mail: haegele@uni-duesseldorf.de*
[c] *Bruker Analytik GmbH, Silberstreifen, D-76287 Rheinstetten, Germany*

Received 28th March 2001, Accepted 5th October 2001
First published as an Advance Article on the web 27th November 2001

The ^{31}P and ^{199}Hg spectra of the new subvalent [*triangulo*-Hg_3]$^{4+}$ based clusters [Hg_3(μ-mdppm)$_3$](O_3SCF_3)$_4$ (**1a**; mdppm = $Ph_2PCH(Me)PPh_2$), which is formed stereoselectively with a *syn–anti–anti* orientation of the methyl groups, and [Hg_3(μ-dppa)$_3$](O_3SCF_3)$_4$ (**4**; dppa = $Ph_2PNHPPh_2$) are successfully simulated with the program WIN-DAISY. By use of the parameters derived from **1a** and **4** the spectra of the parent system [Hg_3(μ-dppm)$_3$](O_3SCF_3)$_4$, which show a very complex pattern, are for the first time completely analysed. The simplification of the spectral pattern in **1a** or **4** compared to [Hg_3(μ-dppm)$_3$](O_3SCF_3)$_4$, respectively, is a result of either symmetry reduction (**1a**) or quasi selective variation of one Hg–P coupling constant (**4**). For $\delta(^{31}P)$, $\delta(^{199}Hg)$, J(HgHg) and the different classes of P–P and Hg–P couplings specific values are found, some of which are powerful tools for the identification of [*triangulo*-Hg_3]$^{4+}$ compounds. The ^1H NMR parameters of **1a**, *anti-* and *syn*-[Hg_3(μ-dpam)(μ-mdppm)$_2$](O_3SCF_3)$_4$ (**2a**, **2b**; dpam = $Ph_2AsCH_2AsPh_2$), [Hg_3(μ-dpam)$_2$(μ-mdppm)](O_3SCF_3)$_4$ (**3**) and [Hg_3(μ-dpam)$_3$](O_3SCF_3)$_4$ lead to a rational interpretation of conformation dynamics in these systems: The three five-membered rings formed by the edges of the [*triangulo*-Hg_3]$^{4+}$ cluster and the three bridging ligands adopt C-envelope conformations in a way that two of the flaps are oriented above and one below the Hg_3 plane, and *vice versa*. The mdppm ligands feature a rigid conformation with an equatorial methyl group and an axial hydrogen atom at the flap carbon atom. The methylene carbon atom of the dpam ligands is able to flip between two positions above and below the Hg_3 plane, if the relative orientations of the three flaps mentioned above are retained. The overall found rigid conformation of the bridging mdppm ligand allows a qualitative estimation of relative thermodynamic preferences of isomers resulting from *syn* or *anti* orientation of mdppm methyl groups.

Introduction

Many compounds containing a [M_3(μ-LL)$_3$] subunit, where M is Ni,[1] Pd,[2] Pt,[3] Cu,[4] Ag,[5] Au[6] or Hg[7] and LL is dppm or a related bidendate ligand,[8] have been synthesised during the last three decades. These complexes have attracted considerable attention due to their role as anion recognition hosts,[2c,d,4,5,7c,e] in view of their photophysical properties[2b,4a,b,9] and because of their catalytic activity.[1,3,10] Whereas these compounds are well characterised in the solid state by single crystal X-ray diffraction, the reported solution NMR data are restricted to ^1H, ^{31}P, ^{195}Pt and ^{199}Hg chemical shifts as well as some coupling constants obtained from partial analysis of the spectra or from heteronuclear clusters.[11] Difficulties in analysing, in particular, $^{31}P\{^1H\}$ NMR spectra arise from their complex pattern in the case of compounds involving metal isotopes with $I = \frac{1}{2}$ or from spectra consisting of a single resonance line for compounds containing metal isotopes with $I \neq \frac{1}{2}$. Multinuclear NMR spectroscopy is apparently the most important tool for the structural characterisation of compounds in solution, revealing information about atomic connectivities, molecular conformation, intra- and inter-molecular exchange processes. As the first example for [M_3(μ-dppm)$_3$] type systems we will show for [Hg_3(μ-dppm)$_3$](O_3SCF_3)$_4$, that consequent derivatisation techniques combined with extensive NMR spectroscopic investigations lead to a complete set of ^1H, ^{31}P and ^{199}Hg NMR shifts and coupling constants, which allow an unambiguous identification of such compounds in solution and give insights into their conformation dynamics. The identity of the cluster [Hg_3(μ-dppm)$_3$]$^{4+}$ with an average formal oxidation state of +4/3 for mercury has been established by single crystal X-ray diffraction.[7a,c] Phosphorus-31 and mercury-199 NMR spectroscopy is expected to yield interesting parameters but the analysis of the complex spectra was hitherto unsuccessful. Fig. 1 shows the $^{31}P\{^1H\}$ NMR spectrum of [Hg_3(μ-dppm)$_3$](O_3SCF_3)$_4$. The satellite pattern due to isotopomers containing one ^{199}Hg nucleus consists of a multitude of transitions extended over a range of *ca.* 2000 Hz and emerges from the baseline only by drastic vertical expansion.

First insights into ^{31}P and ^{199}Hg NMR parameters of [Hg_3]$^{4+}$ clusters were gained recently by derivatisation of [Hg_3(μ-dppm)$_3$](O_3SCF_3)$_4$: Systematic substitution of dppm by dpam and $Ph_2PCH_2AsPh_2$ resulted in new compounds with lower P/[Hg_3]$^{4+}$ ratio and reduced symmetry, which enabled a successful analysis of their NMR spectra.[7d]

In this article we report on the synthesis of [Hg_3(μ-mdppm)$_3$](O_3SCF_3)$_4$ (**1a**; Scheme 1) and [Hg_3(μ-dppa)$_3$](O_3-

DOI: 10.1039/b102840p

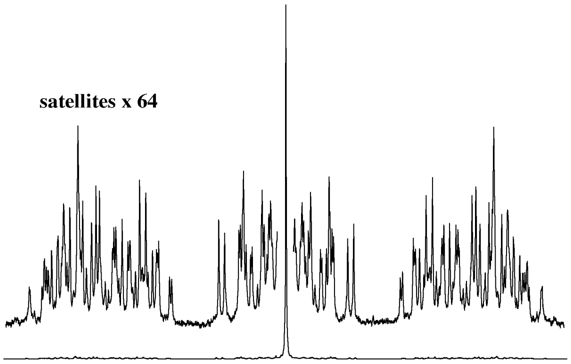

Fig. 1 ^{31}P{^{1}H} NMR spectrum of [$\mathrm{Hg_3(\mu\text{-}dppm)_3}$]($\mathrm{O_3SCF_3}$)$_4$ (center at 54.8 ppm, spectral width 2300 Hz).

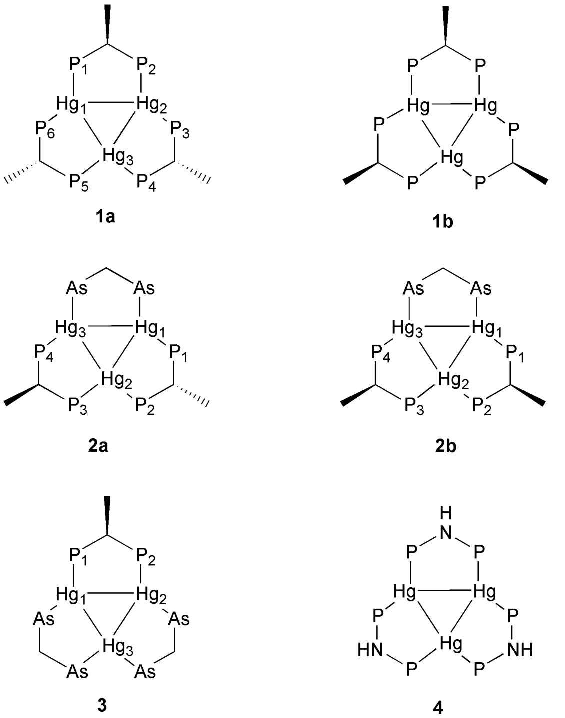

Scheme 1 Structures of the compounds **1a**, **1b**, **2a**, **2b**, **3** and **4**. The charge (4+), phenyl rings and $\mathrm{O_3SCF_3^-}$ anions are omitted for clarity.

SCF$_3$)$_4$ (**4**; Scheme 1). The NMR spectra of both clusters are easier to analyse compared with [$\mathrm{Hg_3(\mu\text{-}dppm)_3}$]($\mathrm{O_3SCF_3}$)$_4$ because of the inequivalence of the phosphorus atoms in the homoleptic complex **1a** (see below) and a favourable constellation of the Hg–P coupling constants of **4**. Using the data of **1a** and **4** enables a successful interpretation of the ^{31}P and ^{199}Hg NMR patterns of [$\mathrm{Hg_3(\mu\text{-}dppm)_3}$]($\mathrm{O_3SCF_3}$)$_4$. Furthermore ^{1}H NMR spectroscopy of the new dpam/mdppm mixed ligand clusters *anti*- and *syn*-[$\mathrm{Hg_3(\mu\text{-}dpam)(\mu\text{-}mdppm)_2}$]($\mathrm{O_3SCF_3}$)$_4$ (**2a**, **2b**; Scheme 1) and [$\mathrm{Hg_3(\mu\text{-}dpam)_2(\mu\text{-}mdppm)}$]($\mathrm{O_3SCF_3}$)$_4$ (**3**; Scheme 1) together with the homoleptic clusters **1a** and [$\mathrm{Hg_3(\mu\text{-}dpam)_3}$]($\mathrm{O_3SCF_3}$)$_4$ reveals detailed information about conformation dynamics of these compounds in solution.

Results and discussion

Syntheses and stereochemistry

[$\mathrm{Hg_3(\mu\text{-}mdppm)_3}$]($\mathrm{O_3SCF_3}$)$_4$ (1a). Compound **1a** is produced stereoselectively by the reaction of [$\mathrm{Hg(Me_2SO)_6}$]($\mathrm{O_3SCF_3}$)$_2$, mdppm and elemental mercury or by treatment of $\mathrm{Hg_2(O_3SCF_3)_2}$ with mdppm according to eqns. (1) or (2), respectively. The cluster **1a** is readily soluble in $\mathrm{CH_2Cl_2}$ or $\mathrm{CH_2Cl_2}$–MeOH (2/1) and is isolated as a yellow microcrystalline powder.

$$2\,[\mathrm{Hg(Me_2SO)_6}](\mathrm{O_3SCF_3})_2 + \mathrm{Hg} + 3\,\mathrm{mdppm} \longrightarrow \mathbf{1a} + 12\,\mathrm{Me_2SO} \qquad (1)$$

$$2\,\mathrm{Hg_2(O_3SCF_3)_2} + 3\,\mathrm{mdppm} \longrightarrow \mathbf{1a} + \mathrm{Hg} \qquad (2)$$

The ^{31}P{^{1}H} NMR spectrum of the isotopomer without ^{199}Hg nuclei (see NMR section) consists of an [ABM]$_2$ pattern (Fig. 2) in contrast to [$\mathrm{Hg_3(\mu\text{-}dppm)_3}$]($\mathrm{O_3SCF_3}$)$_4$ for which a [[A]$_2$]$_3$ spin system gives rise to a single resonance line. The inequivalence of the phosphorus atoms of **1a** is attributed to the relative orientation of the methyl groups of the mdppm ligands, consistent with a *syn–anti–anti* arrangement as shown in Scheme 1. Interestingly, the isomer containing all methyl groups in a *syn* orientation (**1b**, Scheme 1) is not formed at all. We suppose that the exclusive formation of the isomer **1a** is due to the thermodynamic preference of an "all-equatorial" orientation of the methyl groups of the mdppm ligands: All crystal structures of [$\mathrm{Hg_3(\mu\text{-}dppm)_3}$]$^{4+}$ clusters exhibit envelope conformations for the three $\mathrm{Hg_2P_2C}$ five-membered rings with the carbon atom at the flap, two of the flaps are positioned above and one below the $\mathrm{Hg_3}$ plane as sketched in Scheme 2.[7a,c]

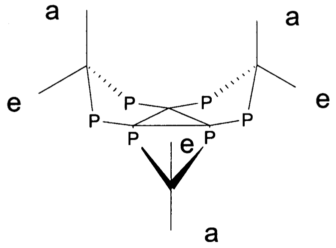

Scheme 2 Conformation of [$\mathrm{Hg_3(\mu\text{-}dppm)_3}$]$^{4+}$ complexes in the solid state (schematic representation); **a** and **e** denote **a**xial and **e**quatorial positions at the envelope carbon atoms.

Each flap bears an equatorial and an axial methylene proton. We propose similar relationships for **1a** and that the equatorial positions are occupied by methyl groups of the mdppm ligands. There is NMR spectroscopic evidence that this also applies for **2a**, **2b** and **3** (see below). For the *syn–syn–syn* isomer **1b** there is no opportunity for an "all-equatorial" arrangement of the methyl groups with a simultaneous C-envelope conformation of the $\mathrm{Hg_2P_2C}$ rings and two of the flaps oriented above and one below the $\mathrm{Hg_3}$ plane.

There is another example of a significant thermodynamic preference of one diastereomer in a Hg/mdppm system reported in the literature: Dean and Srivastava observed the presence of two isomers of [$\mathrm{Hg_2(\mu\text{-}mdppm)_2}$]$^{4+}$ in which two $\mathrm{Hg^{2+}}$ nuclei are bridged by mdppm ligands.[12] The occurrence of isomerism was attributed to *syn* and *anti* arrangements of the methyl groups. An assignment of the ^{31}P signals to *syn* and *anti* isomers could not be made. Equilibrated solutions of [$\mathrm{Hg_2(\mu\text{-}mdppm)_2}$]$^{4+}$ show a ratio [major isomer]/[minor isomer] > 10.

Two other binuclear, doubly bridged metal complexes of mdppm have been prepared: ^{1}H and ^{31}P{^{1}H} NMR data of [$\mathrm{Pd_2(\mu\text{-}mdppm)_2Cl_2}$] revealed the presence of two isomers in a molar ratio of 2/1, of which the major product has been shown by single crystal X-ray diffraction to display an *anti* arrangement of the methyl groups.[13] For [$\mathrm{Ag_2(\mu\text{-}mdppm)_2}$]($\mathrm{BF_4}$)$_2$ ^{31}P{^{1}H} solution NMR data indicate the formation of a sole diastereomer, unfortunately no X-ray crystal structure determination has been performed to establish the relative orientations of the methyl groups.[14]

Mixed ligand [$\mathrm{Hg_3}$]$^{4+}$-clusters with mdppm and dpam. The diastereomeric mixed ligand compounds **2a** and **2b** were formed according to eqn. (3) in a mixture with the two byproducts **1a** (*ca.* 10%) and **3** (*ca.* 10%).

$$2\,[Hg(Me_2SO)_6](O_3SCF_3)_2 + Hg + dpam + 2\,mdppm \longrightarrow \mathbf{2a}, \mathbf{2b} + 12\,Me_2SO \quad (3)$$

The clusters **2a** with the methyl groups in *anti* arrangement and **2b** with the methyl groups in *syn* arrangement are present in a ratio of 2/1. According to ^{1}H NMR results (see below) we presume two energetically degenerate orientations of the methylene group of the dpam ligand in **2a**, whereas only one orientation is present in **2b**. We think that this causes the thermodynamic preference of the diastereomer **2a**.

Compound **3** is formed according to eqn. (4). The clusters

$$2\,[Hg(Me_2SO)_6](O_3SCF_3)_2 + Hg + 2\,dpam + mdppm \longrightarrow \mathbf{3} + 12\,Me_2SO \quad (4)$$

2a and **2b** (together *ca.* 20%) and $[Hg_3(\mu\text{-dpam})_3](O_3SCF_3)_4$ (*ca.* 20%) were identified as byproducts.

The clusters **2a**, **2b** and **3** could not be obtained analytically pure in the solid state and were identified by $^{31}P\{^1H\}$, $^{199}Hg\{^1H\}$ and ^{1}H NMR spectroscopy.

$[Hg_3(\mu\text{-dppa})_3](O_3SCF_3)_4$ (4). Compound **4** was obtained analogously to eqns. (1) and (2) using dppa instead of mdppm. As monitored by ^{31}P NMR spectroscopy, *ca.* 20% of the product is formed besides unidentified Hg(II) complexes. Crystals suitable for a single crystal X-ray structure determination were obtained upon slow evaporation of a $CHCl_3$ solution of **4** prepared analogously to eqn. (2).

^{1}H NMR conformational studies of 1a, 2a, 2b, 3 and $[Hg_3(\mu\text{-dpam})_3](O_3SCF_3)_4$

The compounds **1a**, **2a**, **2b**, **3** and $[Hg_3(\mu\text{-dpam})_3](O_3SCF_3)_4$ with the ligands mdppm and dpam in various stoichiometries exhibit distinctly separated chemical shift ranges for the different aliphatic hydrogen atoms: $\delta(CH)_{mdppm}$ 4.43–4.24, $\delta(CH_2)_{dpam}$ 3.75–3.19, $\delta(CH_3)_{mdppm}$ 1.70–1.50. The H–H and P–H coupling constants do not show any peculiarities, but there are some remarkable features concerning the CH_2-hydrogen atoms of the dpam ligand: Compared with the methine and methyl hydrogen atoms of the mdppm ligand, the methylene protons of dpam show a relatively wide distribution of their chemical shift values. Furthermore the ^3J(HgH) coupling constants for the CH_2-hydrogens in dpam involve values between 0 and 56 Hz whereas for the aliphatic *CH*-hydrogens of mdppm this coupling constant is in all cases too small to be detected. Two assumptions are made for the subsequent discussion to allow a reasonable interpretation for these observations:

1. The Hg_2P_2C and Hg_2As_2C five-membered rings adopt an envelope conformation with the carbon at the flap even in solution (based on crystallographic data of various $[Hg_3(\mu\text{-dppm})_3]^{4+}$ complexes)[7a,c] and
2. The ^3J(Hg–P–C–H)/^3J(Hg–As–C–H) coupling constants show a dihedral angular dependence analogous to the Karplus–Conroy relationship for vicinal ^3J(H–C–C–H) coupling constants (based on the fact that a similar dependence has been observed for ^3J(Pt–P–C–H) couplings in platinum complexes containing dppm as ligand).[15]

Consequently the value of ^3J(Hg–P–C–H)/^3J(Hg–As–C–H) is expected to be approximately 0 Hz for a hydrogen atom in an axial position (φ *ca.* 90°), whereas a hydrogen atom in an equatorial position (φ *ca.* 180°) should exhibit a markedly higher value.

No ^3J(Hg–P–C–H) coupling has been observed for the aliphatic methine protons of the mdppm ligand in the compounds **1a** and **3**. This indicates an axial position for these hydrogen atoms. Consequently compound **1a** adopts a conformation with two carbon atoms of the three five membered rings positioned below and one above the Hg_3-plane. The mdppm *CH*-signals of the compounds **2a** and **2b** could not be analysed due to violent line overlapping but the hydrogen atoms are thought to adopt an axial position as well: This is indicated by their small chemical shift difference compared with the methine protons in compounds **1a** and **3** (<0.2 ppm), whereas the axial and equatorial hydrogen atoms of the dpam CH_2-group in compound **2b** show a chemical shift difference of more than 0.5 ppm (see below).

In contrast to dppm in the complex $[Hg_3(\mu\text{-dppm})_3]^{4+}$ and dpam in $[Hg_3(\mu\text{-dpam})_3]^{4+}$ (see below) the mdppm ligand features a rigid structure in solution, the Hg_2P_2C five-membered ring adopts a C-envelope conformation with an axial methine hydrogen and an equatorial methyl group. A

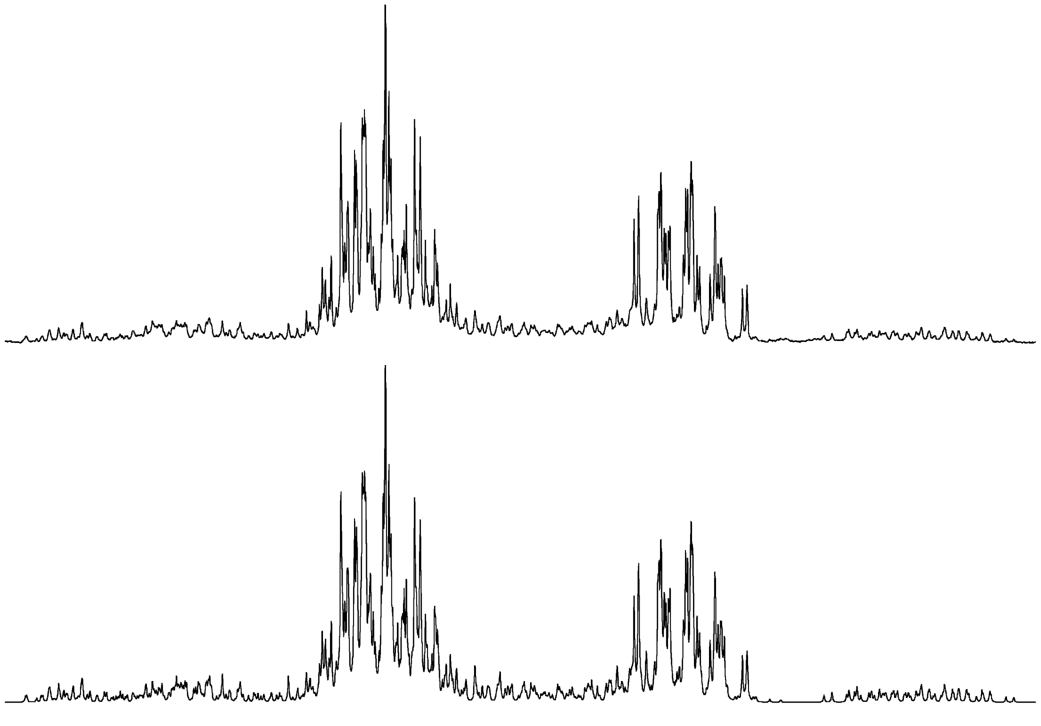

Fig. 2 Experimental (upper trace) and simulated (lower trace) $^{31}P\{^1H\}$ NMR spectrum of **1a** (center at 59.8 ppm, spectral width 3500 Hz).

similar conformation has been found in the crystal structure of *anti*-[Pd_2(μ-mdppm)$_2$$Cl_2$] for the Pd_2P_2C five-membered rings.[13b]

The methylene protons of the dpam ligand in compound **2b** represent an AB system with a chemical shift difference of $\Delta\delta_{AB}$ = 0.56 ppm and two ^3J(Hg–As–C–H) coupling constants having values of 0 and 56 Hz. These observations suggest a rigid conformation of the Hg_2As_2C five-membered ring with fixed positions of the methylene hydrogen atoms. It is most probable that the methylene carbon atom of the dpam ligand in **2b** points to the other side of the Hg_3 plane relative to the methine carbon atoms of the mdppm ligands. The assignment of H^a and H^b is based on this consideration (Scheme 3).

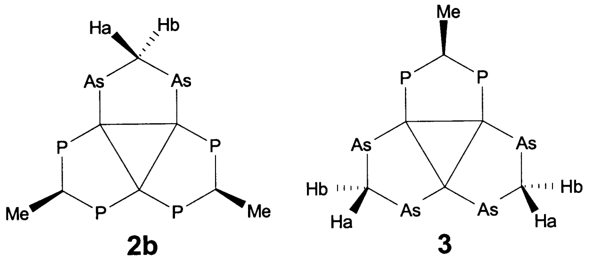

Scheme 3 Assignment of H^a and H^b at the dpam methylene carbon atoms in compounds **2b** and **3** according to Table 3.

As found for the chemical shifts of the axial and equatorial hydrogen atoms in cyclohexane (chair conformation),[16] the axial dpam methylene proton in compound **2b** shows its resonance shifted to lower frequencies with respect to the equatorial proton.

In compound **2a** the chemical shift of the dpam methylene protons and the Hg–As–C–H coupling constant show values of 3.41 ppm and 27 Hz, which approximately coincide with the mean values of $\delta(H^a)/\delta(H^b)$ and $^3J(HgH^a)/^3J(HgH^b)$ in **2b** (3.47 ppm, 28 Hz). This observation is interpreted in terms of a rapid interconversion of the two C-envelope conformations of the Hg_2As_2C five-membered ring, where the methylene carbon atom is placed either below or above the Hg_3 plane. Taking into account the rigid structure for the Hg_2P_2C five-membered rings involving the mdppm ligands, compound **2a** consecutively exhibits a structure with two carbon atoms of the three five-membered rings positioned below and one above the Hg_3-plane.

The dpam methylene protons in compound **3** show Hg–H coupling constants of 16 and 43 Hz. Because of the fixed conformation of the mdppm ligand with the methyl group in an equatorial orientation, there are three possibilities for the two dpam ligands to conform with the structure mentioned above: Both dpam methylene carbon atoms point to the opposite side of the Hg_3-plane relative to the mdppm methine carbon atom (A), or one dpam methylene carbon atom is below and the other above the Hg_3-plane, and *vice versa* (B and C). There are Hg–H couplings of *ca.* 60 Hz and *ca.* 0 Hz expected for conformer A. The structures B and C are anticipated to exhibit a *ca.* 30 Hz coupling for both protons provided for rapid interconversion of B and C. The actual observation of coupling constants of 16 and 43 Hz thus indicates the simultaneous presence of A, B and C, a slightly lower energy content of A compared with B and C and a rapid interconversion of A, B and C on the ^1H NMR time scale. The hydrogen atoms exhibiting a higher axial probability are assigned to H^a (smaller value of ^3J(Hg–As–C–H)), the hydrogen atoms adopting more often an equatorial position are assigned to H^b (higher value of ^3J(Hg–As–C–H)) as indicated in Scheme 3.

The compound [Hg_3(μ-dpam)$_3$](O_3SCF_3)$_4$, present as byproduct in solutions of **3**, features a ^3J(Hg–As–C–H) of 32 Hz. By comparison to the related coupling constants in the compounds **2a**, **2b** and **3** this value leads to the proposal of a rapid interconversion of the six possible conformers (Scheme 4).

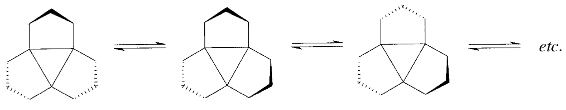

Scheme 4 Proposed conformation dynamics for [Hg_3(μ-dpam)$_3$]-(O_3SCF_3)$_4$ in solution (schematic representation).

The apparent value of ^3J(Hg–As–C–H) is interpreted as the mean of the couplings between mercury and the axial and the equatorial hydrogen, respectively. The same dynamic behaviour proposed for [Hg_3(μ-dpam)$_3$](O_3SCF_3)$_4$ is suggested for [Hg_3(μ-dppm)$_3$](O_3SCF_3)$_4$ (^3J(Hg–P–C–H) = 41 Hz) as well.

The ^1H NMR parameters of the compounds **1a**, **2a**, **2b**, **3** and [Hg_3(μ-dpam)$_3$](O_3SCF_3)$_4$ are collected in Table 1.

Analysis of the ^{31}P and ^{199}Hg NMR spectra

The P–P and Hg–P coupling constants are denoted according to Schemes 5 and 6, respectively.

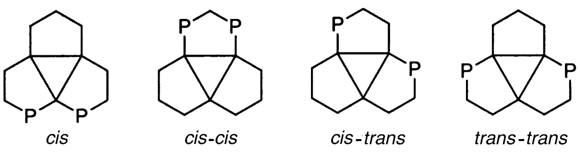

cis *cis-cis* *cis-trans* *trans-trans*

Scheme 5 Stereochemical relations between two P atoms (schematic representation); relations are designated according to the shortest coupling pathway along the Hg_3 framework.

All simulations and iterations were performed by use of the program WIN-DAISY.[17] During the last iteration cycle all

Table 1 ^1H NMR parameters of **1a**, **2a**, **2b**, **3** and [Hg_3(μ-dpam)$_3$](O_3SCF_3)$_4$ [a]

	1a		**2a**	**2b** [b]		**3** [b]		[Hg_3(μ-dpam)$_3$]-(O_3SCF_3)$_4$
$\delta(CH)_{mdppm}$	4.24 (2H)	4.36 (1H)	4.43–4.24	4.43–4.24		4.43		—
$^3J(CH–CH_3)$/Hz	7.6	6.7				7.4		—
$^2J(P–CH)$/Hz	13.4, 13.4	14.1				15.0		—
$\delta(CH_3)_{mdppm}$	1.50 (6H)	1.63 (3H)	1.7–1.5	1.7–1.5		1.70		—
$^3J(P–CH_3)$/Hz	11.4, 11.3	9.8				11.7		—
$\delta(CH_2)_{dpam}$	—		3.41	3.19 (H^a)	3.75(H^b)	3.47(H^a)	3.72(H^b)	3.72
$^2J(H–C–H)$/Hz	—			−11.8	−11.8	−11.9	−11.9	
$^3J(Hg–CH_2)$/Hz	—		27	≈0	56	16	43	32
Solvent	CD_2Cl_2–MeOH (2/1)		CD_2Cl_2	CD_2Cl_2		CD_2Cl_2		CD_2Cl_2

[a] Standard deviations for chemical shifts and coupling constants calculated by the WIN-DAISY automatic routine are ≤0.5 Hz. [b] For assignment of H^a and H^b see Scheme 3.

Table 2 ^{31}P and ^{199}Hg NMR parameters of $[Hg_3(\mu\text{-dppm})_3](O_3SCF_3)_4$, **4** and **1a**[a, b, c]

	$[Hg_3(\mu\text{-dppm})_3](O_3SCF_3)_4$		**4**		**1a**
δ(P)	54.6	54.8	97.6	90.8	61.2 ($P^{1/2}$), 56.4 ($P^{3/6}$), 62.0 ($P^{4/5}$)
$J(PP)_{cis}$/Hz	134.7	135.1	177.4	179.5	127.1 (P^1P^6), 127.0 (P^4P^5)
$J(PP)_{cis\text{–}cis}$/Hz	86.7	86.7	97.9	98.3	100.0 (P^1P^2), 83.7 (P^3P^4)
$J(PP)_{cis\text{–}trans}$/Hz	83.7	83.7	80.3	80.5	81.9 (P^1P^3), 87.7 (P^1P^5), 76.9 (P^3P^5)
$J(PP)_{trans\text{–}trans}$/Hz	22.1	22.0	19.6	19.8	20.5 (P^1P^4), 25.6 (P^3P^6)
δ(Hg)	2576	2576	2577	2577	2571 (Hg^1), 2489 (Hg^3)
^1J(HgP)/Hz	1793	1793	2158	2167	1664 (Hg^1P^1), 1798 (Hg^1P^6), 1927 (Hg^3P^4)
$J(HgP)_{cis}$/Hz	194	194	159	164	156 (Hg^1P^2), 264 (Hg^1P^5), 189 (Hg^3P^3)
$J(HgP)_{trans}$/Hz	1279	1279	1269	1266	1305 (Hg^1P^3), 1208 (Hg^1P^4), 1194 (Hg^3P^1)
J(HgHg)/Hz					16404 ± 63 (Hg^1Hg^3)
Solvent	CD_2Cl_2	CD_2Cl_2–MeOH (2/1)	CD_2Cl_2	CD_2Cl_2–MeOH (2/1)	CD_2Cl_2–MeOH (2/1)

[a] Standard deviations for chemical shifts, P–P and Hg–P coupling constants calculated by the WIN-DAISY automatic routine are ≤0.1 Hz. [b] For the numbering scheme of Hg and P atoms see Scheme 1. [c] For designation of P–P and Hg–P couplings see Schemes 5 and 6.

Table 3 ^{31}P and ^{199}Hg NMR parameters of **2a**, **2b** and **3**[a, b, c]

	2a	**2b**	**3**
δ(P)	61.7 ($P^{1/4}$), 57.9 ($P^{2/3}$)	57.6 ($P^{1/4}$), 60.3 ($P^{2/3}$)	59.6
$J(PP)_{cis}$/Hz	137.7 (P^2P^3)	138.3 (P^2P^3)	—
$J(PP)_{cis\text{–}cis}$/Hz	92.0 (P^1P^2)	84.9 (P^1P^2)	92.4 (P^1P^2)
$J(PP)_{cis\text{–}trans}$/Hz	73.7 (P^1P^3)	67.5 (P^1P^3)	—
$J(PP)_{trans\text{–}trans}$/Hz	31.4 (P^1P^4)	36.0 (P^1P^4)	—
δ(Hg)	2600 ($Hg^{1/3}$), 2385 (Hg^2)	2628($Hg^{1/3}$), 2321(Hg^2)	2412($Hg^{1/2}$), 2663(Hg^3)
^1J(HgP)/Hz	1876 (Hg^1P^1), 2189 (Hg^2P^2)	1882 (Hg^1P^1), 2401 (Hg^2P^2)	2268 (Hg^1P^1)
$J(HgP)_{cis}$/Hz	275 (Hg^1P^2), 163 (Hg^2P^1)	358 (Hg^1P^2), 144 (Hg^2P^1)	234 (Hg^2P^1)
$J(HgP)_{trans}$/Hz	1206 (Hg^1P^3), 1602 (Hg^1P^4)	1149 (Hg^1P^3), 1684 (Hg^1P^4)	1559 (Hg^3P^1)
J(HgHg)/Hz			17361 ± 92 (Hg^1Hg^2) 23499 ± 4 (Hg^1Hg^3)
Solvent	CD_2Cl_2–MeOH (2/1)	CD_2Cl_2–MeOH (2/1)	CD_2Cl_2–MeOH (2/1)

[a] Standard deviations for chemical shifts, P–P and Hg–P coupling constants calculated by the WIN-DAISY automatic routine are ≤0.1 Hz. [b] For the numbering scheme of Hg and P atoms see Scheme 1. [c] For designation of P–P and Hg–P couplings see Schemes 5 and 6.

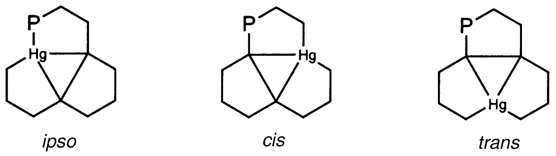

Scheme 6 Stereochemical relations between mercury and phosphorus (schematic representation); relations are designated according to the shortest coupling pathway along the Hg_3 framework, $J(HgP)_{ipso}$ is always denoted as ^1J(HgP) in the text.

spectral parameters (chemical shifts, coupling constants, line widths) were specified as variable. The parameters are collected in Tables 2 and 3.

The $^{31}P\{^1H\}$ spectrum of **1a** may be divided into three subspectra: $[ABM]_2$ (isotopomer without ^{199}Hg nuclei), $[ABM]_2X$ ($^{199}Hg^3$) and AA′BB′MM′X ($^{199}Hg^1$ or $^{199}Hg^2$). Signals arising from subspectra of the isotopomers containing more than one ^{199}Hg are observed in the $^{31}P\{^1H\}$ NMR spectrum but corresponding intensities are too weak for iteration. Although there is a strong overlap of the patterns of the three subspectra the $[ABM]_2$-part could be iterated independently from the other subspectra. By use of these data it was possible to iterate the whole spectrum including all P–P and Hg–P couplings. The assignment of the three sets of phosphorus atoms is based on comparison of the P–P and Hg–P coupling constants with the previously reported compounds $[Hg_3(\mu\text{-dpam})(\mu\text{-dppm})_2](O_3SCF_3)_4$, $[Hg_3(\mu\text{-dpam})_2(\mu\text{-dppm})](O_3SCF_3)_4$, $[Hg_3(\mu\text{-dpam})_2(\mu\text{-}Ph_2AsCH_2PPh_2)](O_3SCF_3)_4$ and $[Hg_3(\mu\text{-}Ph_2AsCH_2PPh_2)_3](O_3SCF_3)_4$.[7d]

The diastereomeric compounds **2a** and **2b** show two $[AB]_2$-systems (isotopomers without ^{199}Hg, ratio 2/1) in the $^{31}P\{^1H\}$ NMR spectrum. The assignment of the chemical shifts of P^1/P^4 and P^2/P^3 is clearly proved by the $[AB]_2X$ and AA′BB′X subspectra in the $^{31}P\{^1H\}$ NMR spectrum (isotopomers containing one ^{199}Hg). The assignment of the ^{31}P and ^{199}Hg NMR parameters are consistent with the appearance of an A_2 and an AB system in the ratio 2/1 for the dpam methylene protons in the ^{1}H NMR spectrum of **2a** and **2b**.

The $^{31}P\{^1H\}$ spectrum of **4** shows a singlet attributable to the $[[A]_2]_3$ spin system of the isotopomer without ^{199}Hg nuclei flanked by widespread mercury satellites (spin system $[AA'A'']_2X$). The satellite patterns attributable to the three different Hg–P coupling constants are well separated. Only regions of the satellite spectrum which are not superimposed by the central singlet were used for the iteration. The spectrum shows also lines of weak intensity, arising from the isotopomer containing two active ^{199}Hg, which were not considered for iteration.

The spin systems of the $^{31}P\{^1H\}$ spectrum of $[Hg_3(\mu\text{-dppm})_3](O_3SCF_3)_4$ are the same as for **4**, but the analysis is more difficult because similar values of ^1J(HgP) and $J(HgP)_{trans}$ cause an overlap of the corresponding patterns of the isotopomer containing one ^{199}Hg nucleus. The analysis of $[Hg_3(\mu\text{-dppm})_3](O_3SCF_3)_4$ succeeded by use of the parameters of **1a** and **4** as starting values. The P–P coupling constants exhibiting the highest and the smallest value were assigned to $J(PP)_{cis}$ and $J(PP)_{trans\text{–}trans}$, respectively.[7d] The assignment of $J(PP)_{cis\text{–}cis}$ and $J(PP)_{cis\text{–}trans}$ results conclusively from symmetry considerations, which were taken into account during the simulation: $J(PP)_{cis\text{–}trans}$ is the only coupling, which appears six times in the complex cation, whereas all other couplings appear only three times. The ^{31}P and ^{199}Hg NMR parameters of $[Hg_3(\mu\text{-dppm})_3](O_3SCF_3)_4$ presented here are the result of the first complete and successful NMR spectroscopic analysis of a $[M_3(\mu\text{-dppm})_3]$ system.

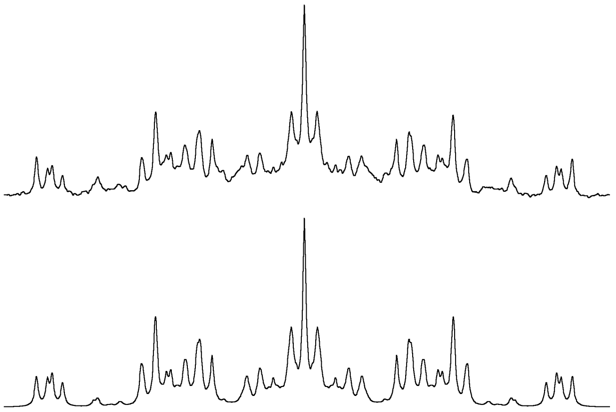

Fig. 3 Experimental (upper trace) and simulated (lower trace) $^{199}Hg\{^1H\}$ NMR spectrum of $[Hg_3(\mu\text{-dppm})_3](O_3SCF_3)_4$ (center at 2576 ppm, spectral width 7300 Hz). Small differences in intensity and lineshape are due to subspectra with more than one active ^{199}Hg in the experimental spectrum, which were not considered in the simulation.

The $^{199}Hg\{^1H\}$ spectra (see Fig. 3 for the $^{199}Hg\{^1H\}$ spectrum of $[Hg_3(\mu\text{-dppm})_3](O_3SCF_3)_4$) of all compounds were simulated by use of the parameters derived from their $^{31}P\{^1H\}$ spectra. For compound **1a** a $^{199}Hg\{^{31}P,^1H\}$ NMR spectrum has been recorded in order to determine the Hg^1–Hg^3 coupling constant from the AB subspectrum of the isotopomer containing two active ^{199}Hg nuclei. The Hg–Hg coupling constants of **3** have been extracted from the $[AX]_2$ and AA′XY ^{199}Hg subspectra of the isotopomers containing two active ^{199}Hg nuclei, respectively.

Discussion of specific ^{31}P and ^{199}Hg NMR parameters

$^{31}P/^{199}Hg$ shifts. The ^{31}P resonances of mdppm in the compounds **1a**, **2a**, **2b** and **3** feature a relatively wide distribution of *ca.* 5 ppm ($\Delta\delta_{mdppm} \approx 63$–$68$ ppm) compared with the related complexes $[Hg_3(\mu\text{-dppm})_3](O_3SCF_3)_4$, $[Hg_3(\mu\text{-dpam})(\mu\text{-dppm})_2](O_3SCF_3)_4$ and $[Hg_3(\mu\text{-dpam})_2(\mu\text{-dppm})](O_3SCF_3)_4$[7d] which exhibit a narrow ^{31}P shift range of *ca.* 1 ppm ($\Delta\delta_{dppm} \approx 77$ ppm). Surprisingly the highest as well as the lowest value is found for compound **1a**. The strongly differing resonance frequencies of $P^{1/4}$ and $P^{2/3}$ in the isomers **2a** and **2b** raised the suggestion that the chemical shift of the phosphorus atoms in one mdppm ligand depends largely on the *syn* or *anti* arrangement of a further mdppm bound to the $[Hg_3]^{4+}$ cluster. In order to evaluate this effect, we took $\delta(^{31}P)$ of compound **3** as the starting parameter and looked at the change in chemical shift upon substitution of a dpam by a mdppm ligand in *syn* (**2b**) or *anti* (**2a**) orientation (Scheme 7). We obtained four increments which were tested for their additivity by calculation of the three phosphorus chemical shifts in compound **1a**. The calculation qualitatively describes the trend of the chemical shifts as evidenced by the series $\delta(P^{4/5}) > \delta(P^{1/2}) > \delta(P^{3/6})$ found in both (experimental and calculated) cases.

The ^{31}P shift of **4** is remarkably solvent dependent and shows values of 97.6 ppm (CH_2Cl_2) or 90.8 ppm (CH_2Cl_2–MeOH, 2/1), respectively.

The ^{199}Hg shifts of all new compounds reported in this article are found in the characteristic range of $[Hg_3]^{4+}$ clusters, exhibiting values markedly downfield relative to arsine or phosphine complexes of mercury(II).[7d] The recently described substituent perturbations for δ(Hg) when replacing an arsine by a phosphine ligand (large positive influence of the *trans* position, smaller negative influence of the *ipso* and *cis* positions, respectively)[7d] are found in the mdppm derivatives of $[Hg_3]^{4+}$ as well as in the related dppm and $Ph_2PCH_2AsPh_2$ complexes, but there exists an additional dependence on the relative orientations of the methyl groups (*syn*, *anti*): Mercury atoms coordinated by two mdppm phosphorus atoms of the ligands in *syn* orientation feature a ^{199}Hg shift distinctly upfield compared to their *anti* analogues. The Hg resonances of the compounds $[Hg_3(\mu\text{-dppm})_3](O_3SCF_3)_4$ and **4** exhibit nearly the same values (in contrast to Hg^2 in **1a**). This may indicate that δ(Hg) is predominantly influenced by steric and not by electronic factors for $[Hg_3]^{4+}$ complexes surrounded by the same atomic donor set.

Coupling constants. The Hg^1–Hg^3 coupling of **1a** amounts to 16404 Hz, the Hg–Hg coupling constants found in **3** feature values of 17361 and 23499 Hz. Similar values were observed for the related compound $[Hg_3(\mu\text{-dpam})_2(\mu\text{-dppm})](O_3SCF_3)_4$.[7d] The Hg–Hg coupling constants in $[Hg_3]^{4+}$ clusters display values (*ca.* 16 to 24 kHz) distinctly separated from other scalar mercury–mercury couplings: One-bond Hg–Hg coupling constants in linear $[Hg_n]^{2+}$ clusters are in the range of 140 to 284 kHz,[18] whereas the largest values for ^nJ(HgHg) ($n > 1$) amount to 8200 Hz.[19]

Comparing ^1J(HgP) in the compounds $[Hg_3(\mu\text{-dppm})_3](O_3SCF_3)_4$ (1793 Hz), **1a** (1796 Hz; mean value) and **4** (2167 Hz), which all bear six phosphorus ligands, the value of **4** containing dppa is markedly increased. It is well known that phosphite complexes of mercury(II) exhibit higher ^1J(HgP) values than their phosphine analogues. The substitution of a phosphorus bound carbon atom by a more electronegative element, *e.g.* N, O, F or Cl, generally leads to larger ^1J(HgP) coupling constants.[20] As one can easily recognise, merely the one-bond Hg–P coupling constant is affected by several hundreds of Hz due to the complete substitution of dppm in $[Hg_3(\mu\text{-dppm})_3](O_3SCF_3)_4$ by dppa in **4**. Since all other couplings are only slightly changed, this corresponds to a quasi selective variation of one Hg–P coupling constant.

The different Hg–P couplings in $[Hg_3]^{4+}$ complexes involving the ligands dpam, dppa, dppm, mdppm and $Ph_2PCH_2AsPh_2$ generally decrease in the order $^1J(HgP) > J(HgP)_{trans} \geqslant J(HgP)_{cis}$, although there is a slight overlap between ^1J(HgP) and $J(HgP)_{trans}$ (Fig. 4).

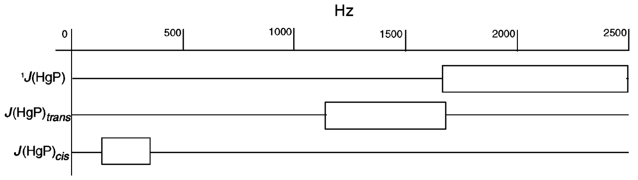

Fig. 4 Ranges for Hg–P couplings in $[Hg_3]^{4+}$ complexes.

The value of $J(PP)_{cis}$ in compound **4** (177.4 Hz) is slightly offset against the values found for **1a**, **2a**, **2b**, $[Hg_3(\mu\text{-dppm})_3](O_3SCF_3)_4$ and $[Hg_3(\mu\text{-dpam})(\mu\text{-dppm})_2](O_3SCF_3)_4$ (146.9–127.0 Hz). This may be caused by the same factors discussed for ^1J(HgP) couplings.[20]

In the complexes $[Hg_3(\mu\text{-dppm})_3](O_3SCF_3)_4$, **1a**, **2a**, **2b** and **4** the values of $J(PP)_{cis\text{–}trans}$ range between 87.7 and 67.5 Hz. If mdppm ligands are in a *syn* orientation the coupling constant seems to be higher than for mdppm ligands in an *anti* orientation. The substitution of a dppm or mdppm ligand in $[Hg_3(\mu\text{-dppm})_3](O_3SCF_3)_4$ or **1a** by dpam, leads to an increase of $J(PP)_{trans\text{–}trans}$.

The value of $J(PP)_{trans\text{–}trans}$ in compound **2a** (*anti*) is higher than in **2b** (*syn*). This effect is also observed for the mdppm ligands in *syn* and *anti* arrangements in compound **1a**.

The values for $J(PP)_{cis}$ and $J(PP)_{trans\text{–}trans}$ in $[Hg_3]^{4+}$ complexes involving the ligands dpam, dppa, dppm, mdppm and $Ph_2PCH_2AsPh_2$ exhibit distinct ranges, which are well separated from other P–P couplings, $J(PP)_{cis\text{–}cis}$ and $J(PP)_{cis\text{–}trans}$ exhibit similar values, but generally *cis–trans* are smaller than *cis–cis* coupling constants (Fig. 5).

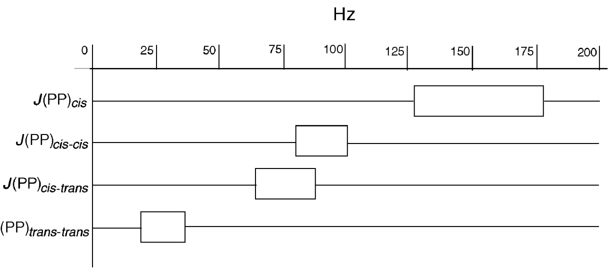

Fig. 5 Ranges for P–P couplings in $[Hg_3]^{4+}$ complexes.

The values of $J(PP)_{cis–trans}$ and $J(PP)_{trans–trans}$ are intriguing because *trans–trans* are smaller than *cis–trans* coupling constants. This observation clearly emphasises that qualitative arguments like *cis* and *trans* relations, which are well established tools for the interpretation of magnitudes of coupling constants in transition metal co-ordination compounds, may not be valid for cyclic structures with unusual bonding geometries. Undoubtedly, there is still some theoretical investigation needed to rationalise the coupling constants in $[Hg_3]^{4+}$ clusters.

Supposing that $^1J(HgP)$ coupling constants have a positive sign,[21] all Hg–P and P–P coupling constants derived from the $^{31}P\{^1H\}$ second order subspectra of the compounds $[Hg_3(\mu\text{-dppm})_3](O_3SCF_3)_4$, **1a**, **2a**, **2b** and **4** are positive. In view of this result, we propose positive values for all Hg–P and P–P coupling constants of the various $[Hg_3]^{4+}$ clusters reported in this article.

Single crystal X-ray structure of 4

Compound **4** crystallises from $CHCl_3$ as colourless prisms containing four solvent molecules per formula unit. An ORTEP[32] plot of the structure is shown in Fig. 6. The $[Hg_3(\mu\text{-dppa})_3]^{4+}$ cation acts as a bifunctional recognition host as has been reported for the $[Hg_3(\mu\text{-dppm})_3]^{4+}$ system[7a,c] and two of the $O_3SCF_3^-$ anions are located inside the two cavities formed by the 12 phenyl groups of the dppa ligands and the Hg_3 triangle. One anion is connected *via* a hydrogen bond to the nitrogen atom of one of the three dppa ligands. The fourth anion bridges between two $[Hg_3(\mu\text{-dppa})_3]^{4+}$ cations *via* two O ··· H ··· N hydrogen bonds (O10 and O12) resulting in an infinite chain structure.

The geometry of the $[Hg_3(\mu\text{-dppa})_3]^{4+}$ system is similar to that of $[Hg_3(\mu\text{-dppm})_3]^{4+}$: Three dppa ligands bridge the edges of the Hg_3 triangle. The Hg–Hg distances are 278.71–282.35 pm compared with 271.7–286.49 pm observed for various $[Hg_3(\mu\text{-dppm})_3]^{4+}$ clusters.[7a,c] The Hg–P distances are 250.6–253.6 pm.

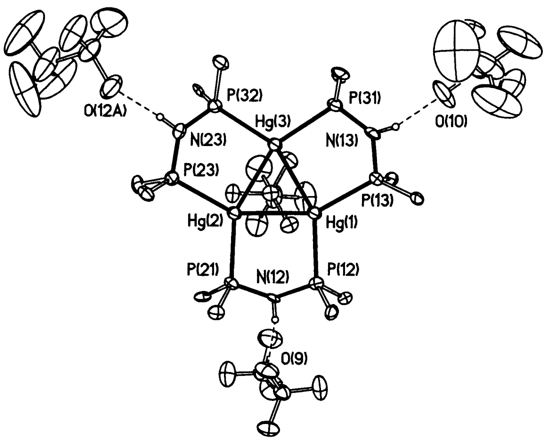

Fig. 6 Molecular structure of **4**. One trifluoromethanesulfonate anion placed above the Hg_3 plane has been omitted for clarity, only the *ipso* carbon atoms of the dppa-bound phenyl groups are shown. The trifluoromethanesulfonate anion containing O(12A) was generated by a symmetry operation from the trifluoromethanesulfonate anion containing O(10).

The P–N distances (165.3–169.2 pm) show values between a P–N single bond (177 pm) and a P–N double bond (156 pm) in phosphacenes as has been reported for other dppa complexes.[22] The five-membered Hg_2P_2N rings formed by the bridging dppa ligands and one edge of the Hg_3 triangle adopt envelope conformations with the nitrogen atoms at the flap. Just as observed for $[Hg_3(\mu\text{-dppm})_3]^{4+}$ clusters, two flaps are oriented below the Hg_3 plane and one above. Two of the Hg–O separations are within the lower Hg–O van der Waals limit of 290 pm based on a Hg radius of 150 pm, and all Hg–O contacts are below the value of 313 pm based on a mercury radius of 173 pm. The N–H ··· O distances are 278.0–283.9 pm. Hydrogen bond interactions concerning anions or solvent molecules, respectively, were previously observed in various dppa complexes.[23] In compound **4** two of the hydrogen atoms attached to the nitrogens are found to lie distinctly out of the PNP plane (H12N: 33(9) pm; H23N: 32(12) pm), and this is thought to be caused by the interaction with the anions.

Conclusion and outlook

We succeeded in demonstrating that an unambiguous characterisation of $[Hg_3(\mu\text{-dppm})_3](O_3SCF_3)_4$ and related subvalent $[Hg_3]^{4+}$ clusters in solution is possible by multinuclear NMR spectroscopy. In comparison with the single crystal X-ray data in the solid state, we obtained additional information about

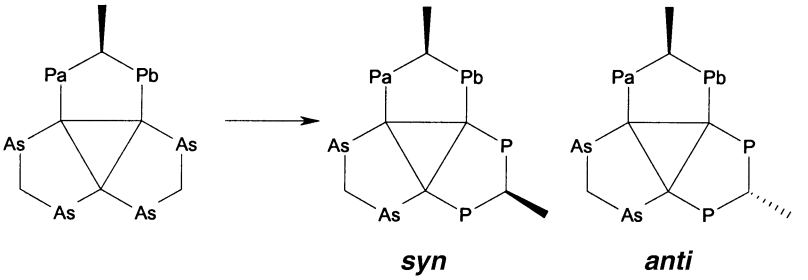

	syn	*anti*
Pa	-2.0	+2.1
Pb	+1.7	-1.7

P atoms in 1a	starting value	P^a_{syn}	P^a_{anti}	P^b_{syn}	P^b_{anti}	Calc.	Exp.
$P^{1/2}$	59.6	-	+2.1	-	-1.7	60.0	61.2
$P^{3/6}$	59.6	-2.0	-	-	-1.7	55.9	56.4
$P^{4/5}$	59.6	-	+2.1	+1.7	-	63.4	62.0

Scheme 7 Effect of the substitution of one dpam ligand in compound **3** by mdppm on the ^{31}P shift and calculation of the ^{31}P shifts of **1a** by the increments obtained (all values in ppm).

the conformation dynamics in these systems. The observed parameters display, in part, unexpected values, which still need theoretical investigations to be rationalised.

The different thermodynamic stabilities of diastereomeric mdppm bridged $[Hg_3]^{4+}$ complexes could be attributed to the rigid C-envelope conformation of the five-membered rings formed by two metal atoms and the P–C–P backbone of the ligand with the methyl group oriented in the less sterically crowded equatorial position. This explanation may also be valid for other complexes containing more than one bridging mdppm ligand.[12–14]

Complete exchange of dppm by mdppm in $[M_3(\mu\text{-dppm})_3]$ type compounds seems to be a promising derivatisation technique for such systems in order to obtain information about their ^{31}P NMR parameters. The preferential formation of the less symmetrical *syn–anti–anti* isomer and the comparatively large effects of the relative ligand orientation on the ^{31}P shift are a good basis for getting spectra, which are accessible for partial analysis and which may in turn be successfully simulated.

The synthesis of mixed ligand diarsine–diphosphine complexes might also be a good tool for making accessible ^{31}P NMR parameters for $[M_3(\mu\text{-dppm})_3]$ compounds or higher nuclearity clusters bearing chemically equivalent dppm ligands. Especially for $[Hg_3]^{4+}$ the existence of mixed ligand compounds could *a priori* not be predicted, because it is well known that mercury complexes bearing different ligands often undergo symmetrisation reactions.

The more pronounced influence of substituents at the phosphorus atom on $^1J(HgP)$ coupling constants compared to couplings involving more than one bond might be a more general phenomenon for M–P couplings in transition metal clusters. There are certainly extensive investigations necessary to verify this thesis.

The interpretation of our ^1H NMR spectroscopic results concerning the protons at the envelope carbon atom of the ligand backbone can help to rationalise ^1H NMR data found for other $[M_3(\mu\text{-dppm})_3]$ type compounds.

At least we propose $[Hg_3]^{4+}$ clusters being interesting subjects for ^{199}Hg solid state NMR spectroscopy, which has received increasing interest in the past few years: Extensive investigations have been performed for Hg(II) compounds,[24] two reports involve Hg(I).[25] Solid state NMR spectroscopy should yield additional information to solution NMR data which could be used to probe structure and bonding. For example, determination of the ^{199}Hg shielding tensor for a variety of $[Hg_3]^{4+}$ compounds could give insights into orbitals contributing to the bonding in such compounds. Besides the subvalent mercury clusters stabilised by bridging phosphine and arsine ligands, there are two examples of this class of compounds existing merely in a crystal lattice, these are the mineral terlinguait, $Hg_4Cl_2O_2$, and $Hg_9As_4O_{16}$.[26,27] For these two species solid state NMR spectroscopy represents the sole method for getting information about their ^{199}Hg data.

Experimental

Materials

$[Hg(Me_2SO)_6](O_3SCF_3)_2$, dpam and mdppm were prepared according to published procedures.[13b,28,29] The syntheses of $[Hg_3(\mu\text{-dppm})_3](O_3SCF_3)_4$ and $[Hg_3(\mu\text{-dpam})_3](O_3SCF_3)_4$ have been described previously.[7a,d] All other chemicals were purchased from commercial suppliers and used without further purification. Elemental analyses were performed by the Institut für Physikalische Chemie, Universität Wien.

Syntheses

$[Hg_3(\mu\text{-mdppm})_3](O_3SCF_3)_4$ (1a). A suspension of HgO (21.7 mg, 0.1 mmol) in H_2O (0.1 ml) was treated with the minimum amount of HO_3SCF_3 (50% in H_2O) to give a clear solution. Elemental mercury (0.1 ml) was added to this solution and the mixture stirred for 30 min. Excess Hg was removed and a solution of mdppm (59.8 mg, 0.15 mmol) in CH_2Cl_2 (0.7 ml) was added and the mixture stirred for 5 min. The CH_2Cl_2 phase was separated, washed twice with H_2O (2 ml) and evaporated *in vacuo* leaving **1a** as a pale yellow microcrystalline powder (93 mg, 78% yield). Anal. calc. for $C_{82}H_{72}F_{12}Hg_3O_{12}P_6S_4$: C, 41.15; H, 3.03. Found: C, 40.95; H, 2.96%.

$[Hg_3(\mu\text{-dppa})_3](O_3SCF_3)_4$ (4). A suspension of HgO (21.7 mg, 0.1 mmol) in H_2O (0.1 ml) was treated with the minimum amount of HO_3SCF_3 (50% in H_2O) to give a clear solution. Elemental mercury (0.1 ml) was added to this solution and the mixture stirred for 30 min. Excess Hg was removed and a solution of dppa (57.8 mg, 0.15 mmol) in $CHCl_3$ (2 ml) was added and the mixture stirred for 5 min. The $CHCl_3$ phase was separated, filtered and left to crystallise by slow evaporation of the solvent. Compound **4** was obtained as colourless crystals (23 mg, 19% yield). Anal. calc. for $C_{76}H_{63}F_{12}Hg_3N_3O_{12}P_6S_4$: C, 38.78; H, 2.70; N, 1.78. Found: C, 38.73; H, 2.71; N, 1.77%.

General procedure for the preparation of solutions of 1a, 2a, 2b, 3, 4 and $[Hg_3(\mu\text{-dppm})_3](O_3SCF_3)_4$ for $^{31}P\{^1H\}$ and $^{199}Hg\{^1H\}$ NMR spectroscopy, for 1a additionally ^1H NMR spectroscopy. $[Hg(Me_2SO)_6](O_3SCF_3)_2$ (48.4 mg, 0.05 mmol) and 0.075 mmol of the ligands in the suitable stoichiometry were dissolved in 0.75 ml solvent (CD_2Cl_2 or CD_2Cl_2–MeOH 2/1) and stirred with elemental mercury (0.1 ml) for 12 hours.

General procedure for the preparation of solutions of 2a, 2b, 3 (with the byproduct $[Hg_3(\mu\text{-dpam})_3](O_3SCF_3)_4$) and $[Hg_3(\mu\text{-dppm})_3](O_3SCF_3)_4$ for ^1H NMR spectroscopy. A suspension of HgO (10.8 mg, 0.05 mmol) in H_2O (0.1 ml) was treated with the minimum amount of HO_3SCF_3 (50% in H_2O) to give a clear solution. Elemental mercury (0.1 ml) was added to this solution and the mixture stirred for 30 min. Excess Hg was removed, 0.75 ml of a CD_2Cl_2 solution of 0.075 mmol of the ligands in the suitable stoichiometry was added and the mixture stirred for 5 min. The CD_2Cl_2 phase was separated, washed twice with H_2O (2 ml) and filtered through cotton wool.

NMR spectroscopy

$^{199}Hg\{^1H\}$, $^{31}P\{^1H\}$ and ^1H NMR spectra were recorded at 20 °C on Bruker DPX 300 or DRX 500 spectrometers. All spectra were recorded using Bruker standard pulse programs, the $^{199}Hg\{^{31}P,^1H\}$ spectrum of compound **1a** was recorded on a Bruker DRX 500 spectrometer by WALTZ 16 decoupling in the spectral region of the ^{31}P signals. The connectivities of the methylene protons in compounds **2b** and **3** could be established unambiguously by ^1H–^1H-COSY spectra. Free induction decays were processed by exponential multiplication (LB-values: 20 [^{199}Hg], 2 [^{31}P] or 0.1 [^1H], respectively) before Fourier transformation, the baselines of the spectra were smoothed by manual baseline correction prior to iteration. Errors in chemical shifts and coupling constants were calculated by the WIN-DAISY automatic routine; these are statistical in nature and probably underestimate the true errors, which also depend on systematic and experimental contributions. $^{31}P/^{199}Hg$ chemical shifts are reported relative to 85% H_3PO_4/2 mmol HgO in 1 ml 60% $HClO_4$, used as an external standard, ^1H chemical shifts are relative to Me_4Si and were determined by reference to the residual ^1H solvent peaks. Coupling constants are reported in Hz.

Crystallography

Crystals of $[Hg_3(\mu\text{-dppa})_3](O_3SCF_3)_4 \cdot 4CHCl_3$ were obtained upon slow evaporation of a solution of $[Hg_3(\mu\text{-dppa})_3](O_3SCF_3)_4$ in $CHCl_3$ at ambient temperature. A colourless prismatic crystal with dimensions 0.7 × 0.65 × 0.5 mm was mounted on a glass fibre, X-ray data were collected at 213(2) K on a Siemens P4 diffractometer (Mo-Kα radiation, monochromator: Highly oriented graphite crystal, ω-scan method). Unit cell parameters were determined and refined from 30 randomly selected reflections in the θ-range between 5.3 and 12.5°, obtained by P4 automatic routine. Crystal system: Monoclinic, space group: $P2_1/n$ (no. 14), unit cell dimensions: $a = 1880.9(4)$, $b = 2190.0(9)$, $c = 2508.0(5)$ pm, $\alpha = 90°$, $\beta = 95.81(2)°$, $\gamma = 90°$. 9668 reflections—8684 of which were independent (R_{int} = 0.0347)—were collected in the θ-range between 3.04 and 19.99° (index ranges: $0 \le h \le 18$, $-1 \le k \le 21$, $-22 \le l \le 22$). Every 97 reflections 3 standard reflections were measured. Data were corrected for Lorentz-polarisation and absorption effects (ψ-scans). The structure was solved by direct methods and subsequent difference Fourier techniques (SHELXS-86),[30] refinement was carried out by full-matrix least-squares methods (SHELXL-93).[31] All non-hydrogen atoms were refined anisotropically. The amine hydrogen atoms were fixed to a distance of 85 pm and refined with isotropic parameters, all other hydrogen atoms were placed at calculated ideal positions (riding model). One solvent molecule is disordered about the C8–H8 axis over two positions (Cl10–Cl12/Cl1A–Cl3A) with occupancies 2/1. Final R indices are $R1 = 0.0360$, $wR2 = 0.0752$ ($I > 2\sigma(I)$) and $R1 = 0.0581$, $wR2 = 0.0865$ (all data).

CCDC reference number 154492.

See http://www.rsc.org/suppdata/dt/b1/b102840p/ for crystallographic data in CIF or other electronic format.

Acknowledgements

Financial support from the Fonds zur Förderung der wissenschaftlichen Forschung, Project P 11842-PHY is gratefully acknowledged.

References

1 (*a*) D. A. Morgenstern, R. E. Wittrig, P. E. Fanwick and C. P. Kubiak, *J. Am. Chem. Soc.*, 1993, **115**, 6470; (*b*) D. A. Morgenstern, C. C. Bonham, A. P. Rothwell, K. V. Wood and C. P. Kubiak, *Polyhedron*, 1995, **14**, 1129.

2 (*a*) L. Manojlovic-Muir, K. W. Muir, B. R. Lloyd and R. J. Puddephatt, *J. Chem. Soc., Chem. Commun.*, 1983, 1336; (*b*) R. Provencher, K. T. Aye, M. Drouin, J. Gagnon, N. Boudreault and P. D. Harvey, *Inorg. Chem.*, 1994, **33**, 3689; (*c*) T. Zhang, M. Drouin and P. D. Harvey, *Chem. Commun.*, 1996, 877; (*d*) P. D. Harvey, K. Hierso, P. Braunstein and X. Morise, *Inorg. Chim. Acta*, 1996, **250**, 337.

3 (*a*) G. Ferguson, B. R. Lloyd and R. J. Puddephatt, *Organometallics*, 1986, **5**, 344; (*b*) R. J. Puddephatt, L. Manojlovic-Muir and K. W. Muir, *Polyhedron*, 1990, **9**, 2767; (*c*) B. T. Sterenberg, M. C. Jennings and R. J. Puddephatt, *Organometallics*, 1999, **18**, 3737.

4 (*a*) J. K. Bera, M. Nethanji and A. G. Samuelson, *Inorg. Chem.*, 1999, **38**, 218; (*b*) J. K. Bera, M. Nethanji and A. G. Samuelson, *Inorg. Chem.*, 1999, **38**, 1725; (*c*) B. F. Straub, F. Rominger and P. Hofmann, *Inorg. Chem.*, 2000, **39**, 2113.

5 (*a*) A. A. M. Aly, D. Neugebauer, O. Orama, U. Schubert and H. Schmidbaur, *Angew. Chem., Int. Ed. Engl.*, 1978, **17**, 125; (*b*) D. Franzoni, G. Pelizzi, G. Predieri, P. Tarasconi, F. Vitali and C. Pelizzi, *J. Chem. Soc., Dalton Trans.*, 1989, 247; (*c*) V. W.-W. Yam, W. K.-M. Fung and K.-K. Cheung, *Chem. Commun.*, 1997, 963; (*d*) V. G. Albano, C. Castellari, M. C. Iapalucci, G. Longoni, M. Monari, A. Paselli and S. Zacchini, *J. Organomet. Chem.*, 1999, **573**, 261.

6 J. W. A. van der Velden, J. J. Bour, R. Pet, W. P. Bosman and J. H. Noordik, *Inorg. Chem.*, 1983, **22**, 3112.

7 (*a*) B. Hämmerle, E. P. Müller, D. L. Wilkinson, G. Müller and P. Peringer, *J. Chem. Soc., Chem. Commun.*, 1989, 1527; (*b*) A. Knoepfler, E. Ellmerer-Müller, K.-H. Ongania, K. Wurst and P. Peringer, *J. Chem. Soc., Dalton Trans.*, 1997, 1607; (*c*) A. Knoepfler-Mühlecker, B. Scheffter, H. Kopacka, K. Wurst and P. Peringer, *J. Chem. Soc., Dalton Trans.*, 1999, 2525; (*d*) A. Knoepfler-Mühlecker, W. Schuh, B. Scheffter, H. Kopacka, K. Wurst and P. Peringer, *Inorg. Chim. Acta*, 2000, **303**, 70; (*e*) B. Scheffter, W. Schuh, K.-H. Ongania, H. Kopacka, R. Malleier, K. Wurst and P. Peringer, *Polyhedron*, 2000, **19**, 871.

8 J. T. Mague, *J. Cluster Sci.*, 1995, **6**, 217.

9 (*a*) W. R. Mason, *Inorg. Chem.*, 1997, **36**, 1167; (*b*) H. Kunkely and A. Vogler, *Chem. Phys. Lett.*, 1993, **206**, 467.

10 P. Braunstein, R. Devenish, P. Gallezot, B. T. Heaton, C. J. Humphreys, J. Kervennal, S. Mulley and M. Ries, *Angew. Chem., Int. Ed. Engl.*, 1988, **27**, 927.

11 P. Braunstein, C. de Méric de Bellefon and M. Ries, *Inorg. Chem.*, 1988, **27**, 1338.

12 P. A. W. Dean and R. S. Srivastava, *Can. J. Chem.*, 1985, **63**, 2829.

13 (*a*) G. Besenyei, C.-L. Lee, Y. Xie and B. R. James, *Inorg. Chem.*, 1991, **30**, 2446; (*b*) C.-L. Lee, Y.-P. Yang, S. J. Rettig, B. R. James, D. A. Nelson and M. A. Lilga, *Organometallics*, 1986, **5**, 2220.

14 A. F. M. J. van der Ploeg and G. van Koten, *Inorg. Chim. Acta*, 1981, **51**, 225.

15 (*a*) F. Neve, M. Ghedini, A. Tiripicchio and F. Ugozzoli, *Organometallics*, 1992, **11**, 795; (*b*) G. J. Arsenault, L. Manojlovic-Muir, K. W. Muir, R. J. Puddephatt and I. Teurnicht, *Angew. Chem., Int. Ed. Engl.*, 1987, **26**, 86; (*c*) A. T. Hutton, C. R. Langrick, D. M. McEwan, P. G. Pringle and B. L. Shaw, *J. Chem. Soc., Dalton Trans.*, 1985, 2121; (*d*) R. J. Puddephatt and M. A. Thomson, *Inorg. Chem.*, 1982, **21**, 725; (*e*) A. Blagg, A. T. Hutton, P. G. Pringle and B. L. Shaw, *J. Chem. Soc., Dalton Trans.*, 1984, 1815.

16 (*a*) F. R. Jensen, D. S. Noyce, C. H. Sederholm and A. J. Berlin, *J. Am. Chem. Soc.*, 1960, **82**, 1256; (*b*) A. G. Moritz and N. Sheppard, *Mol. Phys.*, 1962, **5**, 361.

17 (*a*) U. Weber, R. Spiske, H.-W. Höffken, G. Hägele and H. Thiele, *Manual and Program system, Bruker Manual*, 1993; (*b*) G. Hägele, P. Reinemer and M. Grzonka, *Workshop "Computer in der Chemie", Software-Entwicklung in der Chemie*, 1988, vol. 2, p. 241.

18 (*a*) R. J. Gillespie, P. Granger, K. R. Morgan and G. J. Schrobilgen, *Inorg. Chem.*, 1984, **23**, 887; (*b*) R. Malleier, H. Kopacka, W. Schuh, K. Wurst and P. Peringer, *Chem. Commun.*, 2001, 51.

19 (*a*) G. B. Deacon, M. J. O'Connor and G. N. Stretton, *Aust. J. Chem.*, 1986, **39**, 953; (*b*) J. Eichbichler and P. Peringer, *Chem. Ber.*, 1984, **117**, 1215; (*c*) P. A. W. Dean, J. J. Vittal and M. H. Trattner, *Inorg. Chem.*, 1987, **26**, 4245.

20 C. J. Jameson, in *Phosphorus-31 NMR Spectroscopy in Stereochemical Analysis*, eds. J. G. Verkade and L. D. Quin, VCH, Deerfield Beach, FL, 1987, p. 205.

21 (*a*) I. J. Colquhoun and W. McFarlane, *J. Chem. Soc., Dalton Trans.*, 1981, 658; (*b*) A. Handler, P. Peringer and E. P. Müller, *J. Organomet. Chem.*, 1990, **389**, C23; (*c*) C. A. Ghilardi, S. Midollini, S. Moneti, A. Orlandini and J. A. Ramirez, *J. Chem. Soc., Chem. Commun.*, 1989, 304.

22 N. N. Greenwood and A. Earnshaw, *Chemie der Elemente*, VCH, Weinheim, 1988, p. 698.

23 (*a*) F. A. Knoch and K. J. Meier, *Z. Naturforsch., Teil B*, 1991, **46**, 1699; (*b*) J. Ellermann, F. A. Knoch and K. J. Meier, *Z. Naturforsch., Teil B*, 1990, **45**, 1657; (*c*) J. Ellermann, F. A. Knoch, K. J. Meier and M. Moll, *J. Organomet. Chem.*, 1992, **428**, C44; (*d*) M. Knorr and C. Strohmann, *Eur. J. Inorg. Chem.*, 1998, 495.

24 G. A. Bowmaker, R. K. Harris and S.-W. Oh, *Coord. Chem. Rev.*, 1997, **167**, 49.

25 (*a*) G. A. Bowmaker, R. K. Harris and D. C. Apperley, *Inorg. Chem.*, 1999, **38**, 4956; (*b*) R. A. Santos and G. S. Harbison, *J. Am. Chem. Soc.*, 1994, **116**, 3075.

26 (*a*) S. Scavnicar, *Acta Crystallogr.*, 1956, **9**, 956; (*b*) K. Aurivillius and L. Folkmarson, *Acta Chem. Scand.*, 1968, **22**, 2529; (*c*) K. Brodersen, G. Göbel and G. Liehr, *Z. Anorg. Allg. Chem.*, 1989, **575**, 145.

27 A. L. Wessels, W. Jeitschko and M. H. Möller, *Z. Naturforsch., Teil B*, 1997, **52**, 469.

28 P. Peringer, *J. Inorg. Nucl. Chem.*, 1980, **42**, 1501.

29 A. M. Aguiar, J. T. Mague, H. J. Aguiar, T. G. Archibald and B. Preiean, *J. Org. Chem.*, 1968, **33**, 1681.

30 G. M. Sheldrick, SHELXS-86: Program for crystal structure solutions, Göttingen, 1986.

31 G. M. Sheldrick, SHELXL-93: Program for refinement of crystal structures, Göttingen, 1993.

32 C. K. Johnson, ORTEP, Report ORNL-5138, Oak Ridge National Laboratory, Oak Ridge, TN, 1976.